0605

Pressure Dependence of the CO_2 Contact Angle on Bituminous Coal and Semi - Anthracite in Water

Nikolai Siemons, Hans Bruining, Karl-Heinz Wolf and Willem-Jan Plug

Faculty of Civil Engineering and Geotechnology, Delft University of Technology, the Netherlands

ABSTRACT

Carbon dioxide (CO_2) injection into coal layers serves the dual purpose to enhance coal bed methane production (ECBM) and to store CO_2. The efficiency of this process is expected to be much higher if water is the non-wetting phase in the coal-water-gas system. Therefore, carbon dioxide contact angles in two coal-water-CO2 systems have been measured. The captive bubble technique was used within a pressure range from atmospheric pressure and 140 bar at a constant temperature of 45° C.

Two sets of measurements have been performed, one on a polished semi-anthracite, the second set on a polished high volatile bituminous B coal sample. For the anthracite the following observations have been made. At atmospheric pressure, the contact angle of a CO_2 droplet increases with time, but stays below 90°. At higher pressures (>3 bar) the contact angle increases beyond 90°. This shows that the semi-anthracite coal sample behaves CO_2-wet at system pressures above 3 bar.

CO_2 contact angles on the bituminous coal sample show a different behavior. In the pressures range from atmospheric to 85 bar, CO_2 contact angles are independent of pressure and exhibit values of around 85°. At pressures beyond 100 bar, the coal surface becomes CO_2 wet. The bituminous coal sample is water wet up to much higher pressures than the anthracite. This behavior is related to the difference in stability of the water film between the coal surface and the CO_2. The hydrophobicity of coal increases with rank due to a loss of functional groups which are responsible for hydrogen bonds between coal molecules and water. For the relevant pressures during CO_2 storage, the anthracitic coal behaves CO_2-wet, whereas in bituminous coal the injection pressure has to exceed a pressure of 100 bar in order to wet the coal surface.

It can be concluded that the efficiency of carbon dioxide injection and retention in coal strongly depends on surface properties of the prevailing coal.

INTRODUCTION

One of the promising methods to reduce the discharge of the "greenhouse gas" carbon dioxide (CO_2) into the atmosphere is its sequestration in unminable coal seams. A typical procedure is the injection of carbon dioxide via deviated wells drilled inside the coal seams. After an extensive dewatering phase, carbon dioxide is injected and flows mainly through the fracture system of the coal seam. From there it diffuses through smaller fractures and is subsequently adsorbed in the matrix blocks containing methane. Carbon dioxide displaces methane (CH_4) adsorbed on the internal surface of the coal and the liberated methane is gathered through a production well whereas carbon dioxide remains adsorbed in the coal. This process, known as carbon dioxide-enhanced coal bed methane (CO_2-ECBM), produces natural gas and at the same time reduces emissions of CO_2.

Coal exhibits an extensive fracturing system called the cleat system, in which it is possible to discern a number of cleat systems at different scales. The matrix blocks between the smallest cleat system have

diameters of a few tens of microns [1]. If the cleat system is filled with water, the CO_2 molecular diffusion rate is small (D ~ $2x10^{-9}$ m²/s) and independent of pressure. If the cleat system is filled with gas the diffusion rate is much larger i.e. D ~ $1.7x10^{-7}$ m²/s at 100 bar [2]. It is expected that the smaller cleat network is filled with water if the coal-water-gas system is water-wet and filled with gas if water is the non-wetting phase. We therefore assert that wetting behavior plays an important role in CO_2-ECBM production. Moreover, the presence of water impedes the process of gas adsorption [3, 4, 5]. For this reason we have undertaken an experimental study of the wetting behavior of a coal-water-CO_2 system as a function of pressure. It can be asserted that the exposed coal surface originally formed the bounds of a cleat.

Contact angle measurements provide a simple method to characterize the interfacial energies of a solid in contact with fluids and thus the wetting behavior [6]. In general, these measurements are performed by direct observations of drops deposited on the solid, and viewed from one side. Overview articles describe in detail various technical aspects of a set-up that measures droplet shapes [7].

Section 2 describes the experimental set-up that was developed to measure contact angles from atmospheric pressure to 144 bar. Furthermore the sample preparation and experimental procedure are described. This section also explains the image processing procedure to remove artifacts and to enhance the droplet contour line. Section 3 discusses the contact angle measurements in terms of the wetting behavior of the coal. We end with the conclusions.

BACKGROUND

Wetting properties of coal

Investigations of the wettability behavior of coal reported in the literature are largely based on contact angle measurements for the coal-water-air system at atmospheric pressure. Gutierrez et al. [8] found that the contact angle depends on coal rank. They quantified the effect of surface oxidation using the captive bubble technique. In general, three types of surface components can be distinguished i.e. strongly hydrophobic, weakly hydrophobic and hydrophilic. Low rank coals appear to be hydrophilic and coals become increasingly hydrophobic with increasing rank. Murata [9] performed measurements on pressed pellets of pulverized coal. He found that the contact angle depends on the hydrogen and oxygen content of the coal. Keller [10] has summarized literature data [8, 9, 11, 12,] on the coal-water-air system. The contact angles appear to be largely in the range between 60°-90°. Keller [10] is able to represent observed trends in measurements of the contact angle θ by assuming that cosθ is an area weighted average of the cosine of the contact angles on the heterogeneous surface. To our knowledge there are no contact angle measurements of coal at elevated pressures.

The usual problems with contact angle measurements are all encountered with contact angle measurements on coal. First, surface oxidation alters the properties of the coal surface. Gutierrez-Rodriguez et al. [8] and Gutierrez & Aplan [11] observed a contact angle decrease (increased hydrophilic behavior) in a water-air coal system after exposing its surface for several hours to oxygen sparged water. Secondly, the wettability of the coal surface is highly variable due to its heterogeneous composition. Keller [10] found strongly hydrophobic behavior for the paraffinic hydrocarbon fraction, intermediate behavior for the aromatic fraction and strongly water wet behavior for the minerals and water filled pores. However, like in crude-oil-rock-water systems, we expect that the wetting properties depend on the complex chemistry as a whole. The wettability heterogeneity leads to a varying contact angle. Consequently the droplet will have a non-spherical shape and a non-circular three phase contact line. As a result the left and right contact angles observed in a vertical cross-section will be slightly different. However, large variations of contact angles along the three phase contact line lead to a large water-gas interface, which is energetically unfavorable. Therefore the equilibrium droplet shape favors smooth variations along the three phase contact line. This also explains the empirical equation proposed by Keller [10] i.e. the cosine of the contact angle equals a weighted average of the cosines of the contact angles of the components constituting the coal surface.

Effects of surface heterogeneity

Determination of the contact angle puts severe demands on the smoothness of the surface [7, 13, 14]. The contact angle hysteresis i.e. the difference between the advancing and receding angle may be 10° or more for non-smooth surfaces. Joanny & de Gennes [15] point out that the main reasons for contact

angle hysteresis are the surface energy fluctuations related to rough surfaces and chemical heterogeneity. Rough parts of the surface are partially smoothed because the wetting fluid fills the crevices leading to composite surfaces consisting of substrate and the wetting fluid. The same phenomenon is also expected to remove roughness on a very small scale. De Gennes [13] relates the force exerted by the surface heterogeneity on the contact line to the force originating from the distortion of the interface on the contact line. The latter is described as an elastic force proportional to the deviation of the position of the contact line with respect to its unperturbed position. When the surface energy heterogeneity is small there is only one solution and there is no contact angle hysteresis. When the surface energy heterogeneity is sufficiently large there is more than one stable solution and hysteresis is expected. From the analysis it is clear that the solid surface must be smooth. Drelich et al. [16] state that in practice reproducible contact angles on coal can be obtained if the micro-roughness of the coal surface i.e. the height distance between tops and valleys is less than 40-55 nm. Equilibrium contact angles are established after all three phases get in contact with each other.

A number of electrochemical processes are relevant. A water film formed on the coal surface must be ruptured [17, 18, 19] before contact between the carbon dioxide and the coal surface is established. As a result an equilibrium contact angle will only be established after some time. In addition, two aspects that are specific for the coal-carbon dioxide-water system are important. Contact angles between coal and carbon dioxide are expected to be influenced by the adsorption of CO_2 on the surface. According to Gibbs' equation, the surface tension between water and coal decreases due to adsorption on the surface. This would lead to a contact angle increase. Furthermore, to avoid random formation of CO_2 droplets we did not saturate the water with carbon dioxide at the prevailing pressure. As a consequence, however, diffusion of CO_2 into the water phase will occur and the droplet will decrease in size. From the view point of the CO_2 droplet we observe two receding contact angles at the left and right side of the droplet.

EXPERIMENTAL

Sample preparation

Two coal samples have bee used for this study. The Warndt Luisenthal (hvBb) and Selar Cornish (semi-anthracite) sample was mined in the Saar basin in Germany and South Wales respectively. The coal properties are given in Table 1.

Several coal samples were drilled from lumps of coal and cut into small blocks of a few centimeters length using a diamond saw. One side was polished according to a method given elsewhere [8]. The coal samples were wet polished with a series of abrasive papers with a grit from 60 to 1200, followed by polishing with 0.5 μm abrasive alumina powder and a fibrous cloth. Water washing and ultrasonic cleaning finalized each polishing step. The samples were submersed in doubly distilled water and evacuated for 48 h. This procedure allowed the removal of air from the coal pores and water to penetrate the pore system. The coal sample was taken out of the water, built in the sample holder and transferred to the experimental set-up.

Experimental set-up

The experiments were carried out in a pendant drop (PD) cell [20] adapted to perform captive bubble contact angle measurements. The cell itself is a stainless steel tube with a void volume of approximately 16 cm³. Thermally pre-stressed glasses serve as windows at both ends of the cell. Viton O-rings seal between the glasses and the cell. Through the back window, light is provided. An endoscope is placed near the front window. A digital camera with a pixel resolution of 640×400 is mounted on the endoscope and records the images. The cell can withstand pressures up to 600bar at temperatures up to 200°C. This is well beyond the limit of the conditions of interest to us i.e. pressures ranging from 1 bar to 144 bar and a temperature of 45°C. The cell is placed in an insulated air cabinet that provides stable temperatures (±0.2°C). The set-up is connected to a single working piston high-pressure displacement pump. This pump enables water injection into the cell and is used to generate the desired experimental pressure within the system. A capillary tube is connected at the bottom of the cell and serves as a gas injection device. At the end of the capillary, an exchangeable tip with an outer diameter of 1.59mm is mounted. The capillary is connected to a micro-needle valve and a high-pressure gas reservoir. The needle valve restricts the amount of gas transferred from the reservoir to the injection part to control the bubble volume at the end of the tip.

Conduction of experiments

First the PD-cell (see Figure 1) with the coal sample is evacuated while valves 1, 2, and 3 are closed. Then, with the vacuum pump still running, valve 2 is opened and degassed water is slowly injected into the cell. When the cell is completely filled with water, the vacuum pump is switched off. At this point the cell contains water at atmospheric pressure. Valve 1 is opened and degassed water is circulated at atmospheric pressure for eight hours to clean the cell and tubing. A Du-Nouy ring tensiometer was used to measure the surface tension of the injected and produced water, both were found to be 0.054 N /m. Carbon dioxide was flushed via valves 4, 5, 7, and 6 to avoid air contamination in the experiment. If a higher pressure than atmospheric is required, the piston pump is used to increase the water pressure in the cell. Subsequently, the gas reservoir is filled with carbon dioxide via the gas booster and valves 4 and 5 until the pressure exceeds the water pressure in the cell by 10 bar. Finally all valves are closed and the system is allowed to reach thermal equilibrium for 48 hours before it is ready to use. In order to simulate in-situ conditions the set-up was kept at a constant temperature of 45° i.e. above the critical temperature of CO_2 (31.2°C).

For experiments at atmospheric pressure valve 1 remains open. For high pressure experiments this valve is closed. In order to inject small portions of gas, valve 7 is opened and subsequently closed to fill the small volume between valves 3, 6, and 7 with carbon dioxide. Needle valve 3 is then repeatedly opened to allow small amounts of gas to enter the PD-cell. After some time the carbon dioxide becomes visible as a bubble at the end of the tip. The bubble grows until it hits the coal surface. Gas injection is stopped by closing valve 3. The bubble gradually decreases in size. During this process a camera, connected to an endoscope, captures images of the bubble until the bubble has disappeared completely.

A Matlab routine was programmed to convert the images (see Figure 2) into black and white (top-middle), followed by an edge enhancement procedure (top-right). Finally, the images were cropped by a selected set of coordinates (bottom) to magnify the three phase contact line of the top right image. The cropped images were subjected to the following procedure to determine the contact angles. The procedure uses only a few parameters that need to be adjusted. The parameters are chosen such that (1) the white ring due to refraction in the middle part of the bubble is removed, (2) distorted points (due to the shadow of the bubble on the coal surface) are ignored, (3) five adjacent points at the coal water interface at the leftmost part of the image are connected with five adjacent points at the rightmost part to find the base line. For the bottom left image the X- and Y-coordinates of the white pixels are used to calculate the mean coordinates of the left-side curve representing the water-CO_2 interface and also the slope and direction. The same is done for the bottom right image. With these mean coordinates and the slopes with respect to the base line the angles can be calculated (see Figure 2).

EXPERIMENTAL RESULTS

Experiments have been performed at various pressures from atmospheric to ~144 bar. In all experiments the following behavior is observed. When the bubble is released from the tip, it settles at some position at the coal surface which represents an optimum in terms of interfacial and gravitational energy, depending on its size. It is therefore always slightly shifted from a position vertically above the tip. The difference between the right and left contact angle is always less than 10° and usually less than 5°. Contact angles can be measured until the diameter of the bubble drops below 0.3 mm. In a control experiment the coal surface was covered by a coated microscope glass plate and the measured contact angles were about 85° ± 2° in a pressure range from atmospheric pressure to ~140 bar. In all experiments, the bubble disappearance rate is about the same whether the coal surface is covered with a glass plate or not. In particular a disappearance time exceeding 450 minutes was observed in the atmospheric pressure experiments with and without glass plate. In all other experiments the disappearance time is less than 60 minutes.

At atmospheric pressure the following typical sequence of events is observed (see Figure 3). The gas pressure is slightly increased until CO_2 forms a bubble at the top of the tip. The bubble grows to a size of about 2mm diameter and is captured between the tip and the coal surface. The contact angle is about 66°. The bubble size decreases and the contact angle increases up to 77°. The pressure remains constant, but still small amounts of CO_2 are released by the tip. This CO_2 merges with the bubble, which consequently increases in size, while the contact angle decreases. During the first 190 minutes

occasional releases of CO_2 occur and the bubble size fluctuates accordingly. As the CO_2 supply stops, the bubble size decreases and the contact angle reduces to 62°. The bubble size steadily decreases with time until a critical volume is reached at 300 minutes. The bubble is subsequently detached from the tip and is captured by the coal surface above. During a further 220 minutes its size decreases until it disappears. In that period the contact angle slightly increases fluctuating around 84°. The bubble shape is almost spherical throughout the experiment.

At higher pressures the same procedure is used as for the atmospheric experiments. The same sequence of events occurs when the bubble size fluctuates due to occasional releases of CO_2 from the tip. In this period, however, the bubble shows an overall trend of decreasing in size much faster than in the atmospheric experiment. After detachment from the tip, the bubble shrinks much faster than in the atmospheric experiment e.g. for the 2.6 bar experiment with Selar Cornish and Warndt Luisenthal the bubble completely disappears in 60 minutes and 75 minutes respectively. After detachment the bubble is no longer spherical and starts to spread on the coal surface.

For the high pressure (> 2.6 bar) experiments the bubble, after its release from the tip, disappears in around 20-30 minutes. A plot of the disappearance time versus the pressure shows, in spite of large scatter, a trend inversely proportional to the square root of the pressure.

A typical example of the sequence of events in a high pressure (96 bar) experiment is shown in Figure 4. At t = 0 the bubble just touches the coal surface, but is still attached to the tip. A contact angle of about 50° is observed. As time progresses, the contact angle steadily increases as the bubble size decreases. After three minutes the bubble is detached from the tip. The initial contact angle is about 75° and increases in a time span of 6 minutes to 120°. The bubble shrinks during the next 25 minutes until it completely disappears.

Figure 5 shows the contact angles for all 15 experiments with Selar Cornish at the start and the end of the experiment. At the start of the experiments the bubble is still attached to the tip and contact angles below 90° are observed. In all experiments with P>2.6 bar, contact angles larger 90° are observed some ten minutes after the bubble is released. Figure 5 shows these average (between left and right) contact angles just before the bubble becomes too small to be measured. Only for the atmospheric experiment the contact angle remains below 90°. A linear regression analysis using fourteen data points for contact angles, observed at the end of each experiment, was carried out. The square of the correlation coefficient r (Pearson's correlation) is equal to 0.34. The slope for the large contact angles for 95% confidence limits (two times the standard deviation) is 0.17±0.14 degree/bar i.e. a significant increase of the contact angle with pressure. We excluded the atmospheric pressure point in the linear regression analysis because the atmospheric pressure experiment behaves different from all the other experiments. The intercept for the contact angle for P=0 is 111° ± 10.5°, also for 95% confidence limits. The standard deviation for the contact angles with respect to the line obtained by the linear regression method is less than 15°. If the atmospheric pressure point is included we find a stronger positive correlation between pressure and contact angle. Contact angles at the start of the experiment observed in Figure 5 do not show a significant trend with pressure.

Contact angles at the start and the end for sample Warndt Luisenthal are plotted in Figure 6. Both, the start and the end contact angles below 87 bar (Figure 6) don't exhibit a significant trend with pressure. At the start the experiments show contact angles between 35 and 46°. Furthermore, they are more scattered than their corresponding end values exhibiting an average value of 85°. The standard deviation for the start contact angles with respect to the line obtained by the linear regression method is less than 5° and for the end values less than 1.5°.

For experiments exceeding 100 bar, a significant trend with pressure can be recognized. The end contact angles increase with pressure from 124° to 144°. The intercept for the contact angle for P=0 is 87° ± 10.7°. The square of the correlation coefficient r (Pearson's correlation) is equal to 0.42. The slope for the large contact angles for 95% confidence limits (two times the standard deviation) is 0.34 ± 0.11 degree/bar.

DISCUSSION

The reason for the slow disappearance rate of the bubble at atmospheric pressure is not clear. Given the fact that the CO_2 concentration in the gas phase (0.04 mol/l) and the concentration in the liquid phase (0.034 mol/l at P=1 bar) are similar we expect that the characteristic disappearance time τ for a bubble

with a radius R of 1mm can be estimated as $\tau = R^2/D = 10^{-6}/2\times10^{-9}$=500 seconds, independent of pressure. Here D is the diffusion coefficient for CO_2 in water in m²/s. This characteristic time is indeed observed for the high pressure experiments, but at atmospheric pressure the bubble survives much longer (see Figure 3). As the same slow dissolution of the bubble is observed when the coal surface is covered with a glass plate, we conclude that the bubble mainly disappears due to dissolution in the water phase and not due to adsorption on the coal.

The contact angle behavior can be qualitatively understood as follows. Initially the bubble is trapped between the tip and the coal surface. The tip causes a bubble deformation such that the apparent contact angle at the coal surface is smaller than the equilibrium value (Figure 3, Figure 4, Figure 5, Figure 6). As the bubble is released from the tip, the system finds a new equilibrium configuration. Upon its release, the contact spot with the coal surface increases and an advancing contact angle is observed in Figure 4. In most of our experiments the equilibrium configuration is established almost instantaneously. Subsequently the bubble decreases in size due to dissolution and a receding contact angle is observed. However, the difference between the advancing and receding contact angle is small and therefore we conclude that the observed contact angles are a good representation of the equilibrium contact angle.

The CO_2 bubble rests against a surface that consists of coal and patches of water films on the surface. The difference between receding and advancing contact angle on the coal surface is mainly attributed to the existence of these water patches. As the bubble advances it encounters a surface with more water than when the bubble recedes.

The three phase contact line cannot follow the local contact angle behavior on a heterogeneous surface as this would imply a highly irregular water-CO_2 surface with a high surface energy. Therefore it can be expected that the contact angle varies more smoothly. Indeed, the left and right contact angle usually differ less than 5°. It can also be expected that the bubble finds an energetically optimal position that changes with time as the bubble gradually dissolves. As the coal surface consists of hydrophilic mineral parts, initially water filled pores, hydrophobic aliphatic parts and intermediately wet aromatic parts, we expect that the coal surface is on average neither totally water wet nor totally carbon dioxide wet.

For all experiments with Selar Cornish and Warndt Luisenthal the contact angle increases to 111°±10.5° + (0.17±0.14) P [bar] and 78.7±10.7° + (0.34±0.11) P [bar], respectively.

It is unlikely that the interaction of CO_2 with the Selar Cornish coal surface at atmospheric pressure and a pressure of 2.6 bar is completely different. For instance, the interfacial tension between carbon dioxide and water drops from 68mN/m at atmospheric pressure to 60mN/m at 20.7 bar [22]. One explanation is that contact angle hysteresis effects are more pronounced for the experiments where the bubble size decreases more rapidly. Another explanation is that water films at the coal surface remain more stable for the same reason that the dissolution rate for the atmospheric pressure bubble is low. We conclude that for the semi-anthracite used in these experiments the surface is carbon dioxide wet at pressures relevant for carbon dioxide storage in coal layers. Possibly this coal surface is also carbon dioxide wet at atmospheric pressure, but for the duration of the experiment water films prevent the exposure of the coal surface to carbon dioxide. Indeed, the lower rank Warndt Luisenthal coal behaves water wet up to pressures of 87 bar. This behavior can be related to the different surface chemistry of the two coal samples used. Nishino [4] found that the affinity for water depends on functional groups (mainly carboxylic and hydroxyl) groups which are more abundant in a coal of the hvBb rank [8, 23, 24]. Further Plug et al [25] observed the same wettability trends as a function of pressure for identical coal samples using a capillary pressure device.

CONCLUSIONS

- Reproducible contact angles were measured in two water-CO_2-coal system for pressures ranging between atmospheric and 144 bar.
- When the bubble is released from the tip of the injection capillary, the apparent contact angles are below 90°, indicating the influence of the tip on the bubble shape.
- From the behavior of the contact angle of the bubble after its detachment from the tip we conclude that the observed contact angle is a good representation of the equilibrium contact angle.

- At atmospheric pressure the semi-anthracite remains water-wet with contact angles θ of 85°. Above 2.6 bar the contact angle increases with pressure i.e. θ= (111° +10.5°) + (0.17.14) P bar with 95% confidence limits. This shows that Selar Cornish behaves CO_2-wet at pressures above 2.6 bar.
- Sample Warndt Luisenthal changes its wetting behavior towards CO_2 wetting at much higher pressures. The contact angle θ increases with pressure i.e. θ= 78.7±10.7° + (0.34±0.11) P [bar].
- For Selar Cornish It is unlikely that the different behavior of the atmospheric experiment with the higher pressure experiments starting at 2.6 bar is due to a difference in interaction energy between the coal surface and the gas molecules. It is more plausible that this behavior is related to the difference in stability of the water film between the coal and the CO_2.
- At atmospheric pressure the captured CO_2 bubble dissolves in the water in a time span of several hours. At higher pressures (>2.6 bar) dissolution takes place in several tens of minutes. This may suggest that the same mechanism accounts for the stability of the water film (low contact angles) and the slow dissolution rate of the bubble at atmospheric pressure.
- Water film stability may also be the reason for the water-wet behavior of sample Warndt Luisenthal for pressures below 87 bar.
- We conclude that for the Selar Cornish sample the water-CO_2 -coal system is CO_2-wet at all pressures, becoming slightly more CO_2 -wet at higher pressures.
- For the relevant pressures during CO_2 storage semi-anthracitic coal behaves CO_2-wet.
- For CO_2 storage in hvBb coal the injection pressure has to overcome a pressure threshold of 87 bar to carbon dioxide wet the surface.

REFERENCES

1. Gamson P.D., Beamish B.B. and D.P. Johnson (1993):"Coal microstructure and micropermeability and their effects on natural gas recovery", Fuel, 72 p. 87-99.
2. Bird R.B., Stewart W.E. and E.N. Lightfoot, eds., (1960):"Transport phenomena", John-Wiley New York 1960 780 p.
3. Mavor M.J., Owen L.B. and T.J. Pratt (1990):"Measurement and evaluation of coal sorption isotherm data", SPE 65th Annual Technical Conference and Exhibition, September 23-26, New Orleans, Society of Petroleum Engineers, SPE 20728, p. 1-14.
4. Nishino, J., (2001):"Adsorption of water vapor and carbon dioxide at carboxylic functional groups on the surface of coal", Fuel 80, 757–764.
5. Krooss B.M., Bergen F. van, Gensterblum Y., Siemons N., Pagnier H.J.M. and P. David (2002):"High-pressure methane and carbon dioxide adsorption on dry and moisture-equilibrated Pennsylvanian coals", Int. J. Coal Geology, 51, p. 69-92.
6. Adamson A.W. and A.P. Gast, eds, (1990):"Physical chemistry of surfaces", John-Wiley, New York 770p.
7. Spelt J. and E.L Vargha-Butler in: A.W. Neumann, ed., (1996):"Applied surface thermodynamics", Surfactant Science Series 63, 394p.

8. Gutierrez-Rodriguez J.A., Purcell R.J. and F.F. Aplan (1984):"Estimating the hydrophobicity of coal", Colloids Surfaces 12, p. 1-25.
9. Murata T. (1981):"Wettability of coal estimated from the contact angle", Fuel, 60, p. 744-746.
10. Keller D.V. (1987):" The Contact angle of water on coal", Colloids and Surfaces, 22, p. 21-30.
11. Gutierrez-Rodriguez J.A. and F.F. Aplan (1984):"The effect of oxygen on the hydrophobicity and floatability of coal", Colloids Surfaces, 12, p. 27-51.
12. Fuerstenau D.W:"Flotation and selective agglomeration of Western Coals", Office of Surface Mining and Reclamation Enforcement, U.S. Dept. Interior, final report g/79-12/81.
13. Gennes P.G. de (1985):"Wetting; statics and dynamics", Rev. Mod. Phys. 57, 3 part I, p. 827-863.
14. Fox H.W. and W.A. Zisman (1950):"The spreading of liquids on low energy surfaces. polytetrafluoroethylene", J. Coll. Sci., 51, p. 514-531.
15. Joanny J.F. and P.G. de Gennes (1984):"A model for contact angle hysteresis", J. Chem. Phys. 81, p. 552-562.
16. Drelich J., Laskowski J.S., Pawlik M. and S. Veeramasuneni (1997):"Preparation of coal surface for contact angle measurements", J. Adhesion Sci. Technol. 11, p. 1399-1431.
17. Hirasaki G.J. in: N.R.Morrow, ed, (1991):"Interfacial phenomena in petroleum recovery", Dekker, New York, p. 23.
18. Hirasaki G.J. in: N.R.Morrow, ed, (1991):"Interfacial phenomena in petroleum recovery", Dekker, New York, p. 77.
19. Hirasaki G.J. (1991):"Wettability: Fundamental and surface forces", Society of Petroleum Engineers, SPE Journal of Formation Evaluation 17367, p. 217-226.
20. Huijgens R. J. M. (1990):"The Influence of interfacial tension on nitrogen flooding", PhD dissertation, Delft University of Technology 160p.
21. Krevelen D.W. van (1993):"Coal, Typology-Physics-Chemistry-Constitution", Elsevier, Amsterdam, (1993) 493p.
22. Chun B.S. and G.T. Wilkinson (1995):"Interfacial tension in high-pressure carbon dioxide mixtures", Ind. Eng. Chem. Res. 34, p. 4371-4377.

23. Crawford, R.J. Guy, D.W. and D.E. Mainwaring (1994):"The influence of coal rank and mineral matter content on contact angle hysteresis", Fuel 73, p. 742-746.
24. Arnold B.J. and F.F. Aplan (1989):"The hydrophobicity of coal", Fuel 68, p. 651-658.
25. Plug W-J., Mazumder S. Bruining J. And K.H. Wolf (2006):" Capillary Pressure and wettability behavior of the coal-water-carbon dioxide system at high pressures", Paper 0606, 2006 International Coalbed Methane Symposium Alabama, May 22-26.

ACKNOWLEDGMENTS
The research reported in this paper was carried out as part of the project ENK6-CT-00095-ICBM under the ENERGY and SUSTAINABLE DEVELOPMENT PROGRAM founded by the European Commission. The financial support is gratefully acknowledged. We thank L. Vogt for technical support.

TABLES

Table 1: Results of the coal petrology, proximate and ultimate analysis

	Warndt	Selar Cornish
rank	hvBb	Semi-
Vmax [%]	0.71	2.41
Vitrinite [%]	74.4	73.6
Liptinite [%]	15.6	0
Inertinite [%]	9	24.6
Minerals [%]	1	1.8
Volatile Matter (w.f.) [%]	40.5	10.4
Fixed carbon (d.a.f.)	58.6	89.3
Calorific value [MJ/m^3]	-	33.2
Carbon [%]	81.3	85.68
Hydrogen [%]	5.58	3.36
Nitrogen [%]	1.88	1.56
Sulfur [%]	0.69	0.68
Oxygen [%]	5.47	5.58

FIGURES

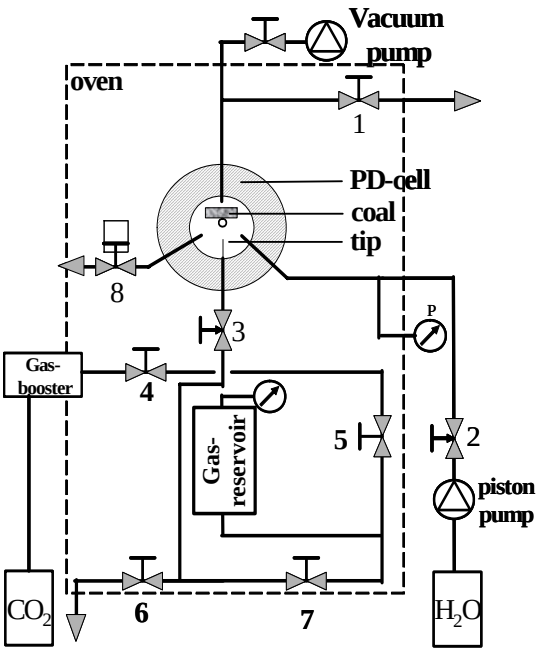

Figure 1: Schematic view of the set-up

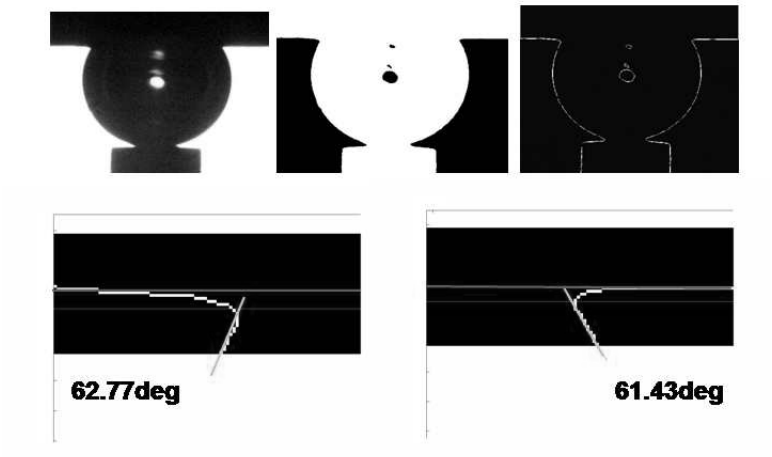

Figure 2: Image processing of a droplet and determination of left and right contact angles. Top left: the raw image. Top middle: the same droplet converted to a black and white image. Top right: droplet after edge enhancement. Below: the magnified image near the three phase contact line and determination of the contact angles. The slope near the surface is attributed to a spurious shadow. Such an abrupt change in curvature would be incompatible with gravity/ capillary pressure equilibrium.

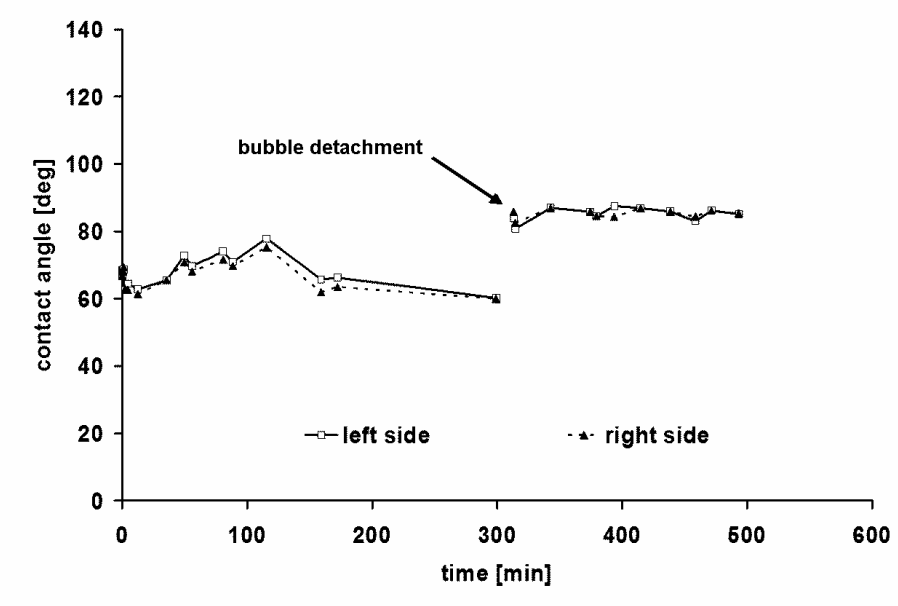

Figure 3: Contact angle history for the atmospheric pressure experiment of sample Selar Cornish. Left and right contact angles are indicated. At the discontinuity the droplet is detached from the tip.

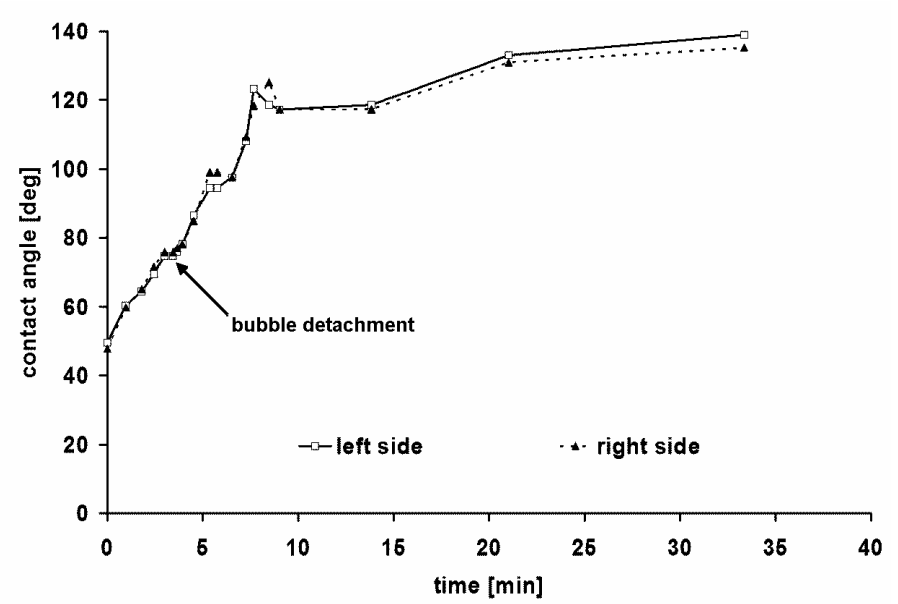

Figure 4: Contact angle history of sample Selar Cornish at 96 bar.

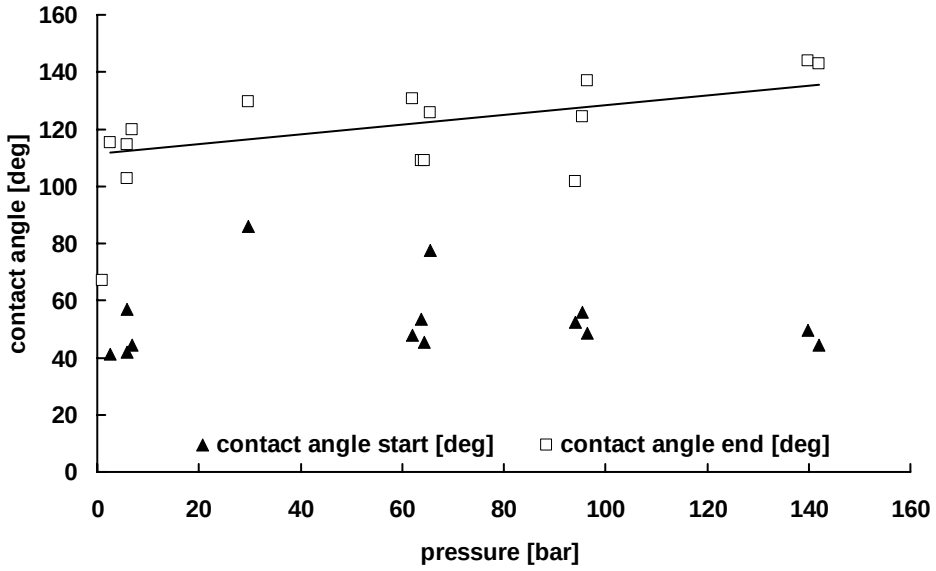

Figure 5: Contact angles on sample Selar Cornish at start and end of the experiments as a function of pressure. Contact angles at the start are all below 90°. Contact angles at the end of the experiment exceed 90°, except for the experiment performed at atmospheric pressure.

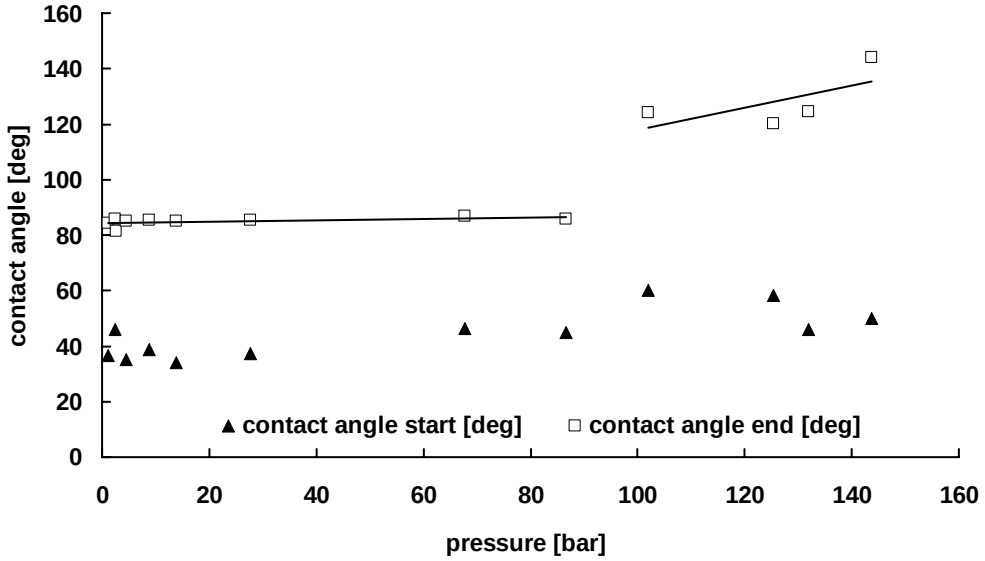

Figure 6: Contact angles on sample Warndt Luisenthal at start and end of the experiments as a function of pressure. Contact angles at the start are all below 60°. Contact angles at the end of the experiment don't exceed 85° for pressures below 90 bar. For pressures beyond 90 bar, the contact angle increases with pressure.